Progress In Electromagnetics Research Letters, Vol. 111, 79–84, 2023

Beam-Pattern Control via Thinned Elements Strategy in Linear and Planar Phased Arrays

Jafar Ramadhan Mohammed*

Abstract—Reconfigurable antenna arrays play a major role in the current and future wireless communication systems due to their multifunctional capabilities and many other advantages. Conventionally, the array pattern reconfigurations were usually achieved by controlling the excitation amplitudes and phases of all or most of the array elements which are generally costly and complex methods. In this paper, a simple method for controlling the reconfigurability of the beam-patterns of linear and planar arrays is presented. It can be easily switched between narrow and wide beams using thinned elements strategy. First, the array elements are divided into three groups based on their locations namely central, middle, and outer elements. Their amplitude weights are chosen to be unity, adaptive, and zero, respectively. To add some desired constraints on the array beam-patterns such as limited sidelobe level and specified nulls placement, the excitation weights of the middle elements are optimized such that an abrupt change in the array taper is avoided. This also avoids an undesired change in the sidelobe pattern. A genetic algorithm is used to perform such optimization so that the produced beam-patterns are best matched to the desired ones. Moreover, the size of the thinned region controls the resulting beam width.

1. INTRODUCTION

Reconfiguration in the array radiation pattern is considered as a major issue for current and future wireless communication systems. It is usually achieved by controlling relative excitation amplitudes and phases of the array elements, for example, see [1–3]. However, such methods were characterized as complex and costly [4–6]. The concept of thinned arrays can be creatively exploited for pattern reconfiguration to operate in different modes according to the demanded applications. In [7], the author introduced the concept of partially thinned elements for null steering, while in [8] the useless elements that had negligible effect on the desired array patterns were thinned out (i.e., turned off). Thinning concept can be included in the array taper such that its effective aperture can be increased or decreased according to the required beam width. In general, array tapering can be defined as the manipulation of the excitation amplitudes of the individual array elements and its contribution to the overall array radiation pattern. Usually, array tapers such as Taylor or Dolph-Chebyshiv were used to reduce the undesirable high sidelobes of the array pattern, but it generally comes at the cost of lower directive gain and widens beam width.

In this paper, the array elements are first divided into three main subsets according to their locations namely central, middle, and outer such that the overall antenna pattern can be easily reconfigured between narrow and wide beam widths with low sidelobe level (SLL) and steered nulls. The narrow beam patterns can be achieved by selecting the amplitude excitations of the central subset elements to be unity, while those for middle and outer subset elements are optimized to get the lowest SLL and steered nulls. On the other hand, the wide beam patterns can be obtained by turning off all the

Received 24 February 2023, Accepted 22 May 2023, Scheduled 3 July 2023
* Corresponding author: Jafar Ramadhan Mohammed (jafar.mohammed@uoninevah.edu.iq).
The author is with the College of Electronics Engineering, Nineveh University, Mosul 41002, Iraq.

elements of the outer subset. That is by setting their excitation amplitudes to zero. In this case, only the excitation amplitudes of the middle subset elements are optimized such that the corresponding wide beam pattern has the lowest SLL and steered nulls. The number of active or passive elements in each subset is determined by the optimization algorithm such that the required patterns are obtained.

2. DESCRIPTION OF THE METHOD

Consider a linear array of even number of elements $N = 2M$ which are symmetrically distributed about the center of the array with equally spaced inter-element spacing of $d = \lambda/2$. Its radiation pattern as a function of the elevation angle (θ) in the far-field region can be written as [9]

$$\mathrm{AF}_{\mathrm{uniform}}(\theta) = \sum_{m=1}^{M} w_m \cos\left[\frac{(2m-1)}{2} kd\sin\theta\right] \tag{1}$$

where $k = \frac{2\pi}{\lambda}$, λ is the wave length, and $w_m = a_m e^{P_m}$ is the complex amplitude and phase excitations of the array elements. For uniformly excited arrays, its taper is $w_m = 1$ for $m = 1, 2, ..., M$. Note that there are abrupt changes in the taper amplitudes at the end elements of both array edges which causes high SLL about -13 dB. The solution to this problem is to apply a specific weighting function across the array taper where the central elements give more weights and the outer elements less weights as most of the well-known tapers such as Dolph-Chebyshiv, Taylor, and many others [7]. To proceed with the proposed multi-region taper, the array elements are divided into three subsets or regions according to their locations and taper amplitudes. The first subset contains a number of elements whose amplitudes are all set to ones which are usually located at the array center. The second subset contains the transition elements whose amplitudes are bounded between ones and zeros which are located at the middle of the array, while the third subset contains only the thinned elements whose amplitudes are zero, and they are located at the array edges. Assume that the numbers of elements in these three subsets are M_1, M_2, and M_3, respectively.

Then, the overall array pattern of these three portioned subsets can be given by

$$\begin{aligned}\mathrm{AF}(\theta)_{\mathrm{taper}} = &\underbrace{\sum_{m_1=1}^{M_1} w_{m_1} \cos\left[\frac{(2m_1-1)}{2} kd\sin\theta\right]}_{\text{Central Subset}} + \underbrace{\sum_{m_2=1}^{M_2} w_{m_2} \cos\left[\frac{(2m_2-1)}{2} kd\sin\theta\right]}_{\text{Middle Subset}} \\ &+ \underbrace{\sum_{m_3=1}^{M_3} w_{m_3} \cos\left[\frac{(2m_3-1)}{2} kd\sin\theta\right]}_{\text{Outer Subset}}\end{aligned} \tag{2}$$

Array pattern reconfigurability is achieved by properly controlling the excitation amplitudes of the central subset elements, a_{m_1}, middle subset elements, a_{m_2}, and the outer subset elements, a_{m_3}. From practical implementation point of view, the amplitude-only method is considered so that the excitation phases, P_m, are solely left for the scanning purpose. Further, we choose $a_{m_1} = 1$ for $m_1 = 1, 2, ..., M_1$ and $a_{m_3} = 0$ for $m_3 = 1, 2, ..., M_3$, while a_{m_2} are variables for the optimization algorithm or the degrees of freedoms that determine the required SLL and the steered nulls. Intuitively, to achieve narrow beam pattern, $M_1 > M_2$ and $M_3 = 0$. Here the number of subset elements M_2 should be large enough to provide sufficient number of degrees of freedom for achieving the required array pattern shape.

To obtain a wide beam pattern, we basically need to shorten the array aperture by switching off more edge elements, thus M_3 should be relatively large and M_1 small while M_2 should be able to provide the necessary degrees of freedom. The genetic algorithm is used to optimally choose the values of M_1, M_2, and M_3 as well as the excitation amplitudes of the middle subset elements.

3. SIMULATION RESULTS

Consider a symmetric linear array with $N = 2M = 40$ radiating elements with half wavelength inter-element spacing. As an example, a narrow beam pattern is achieved with SLL below -30 dB and

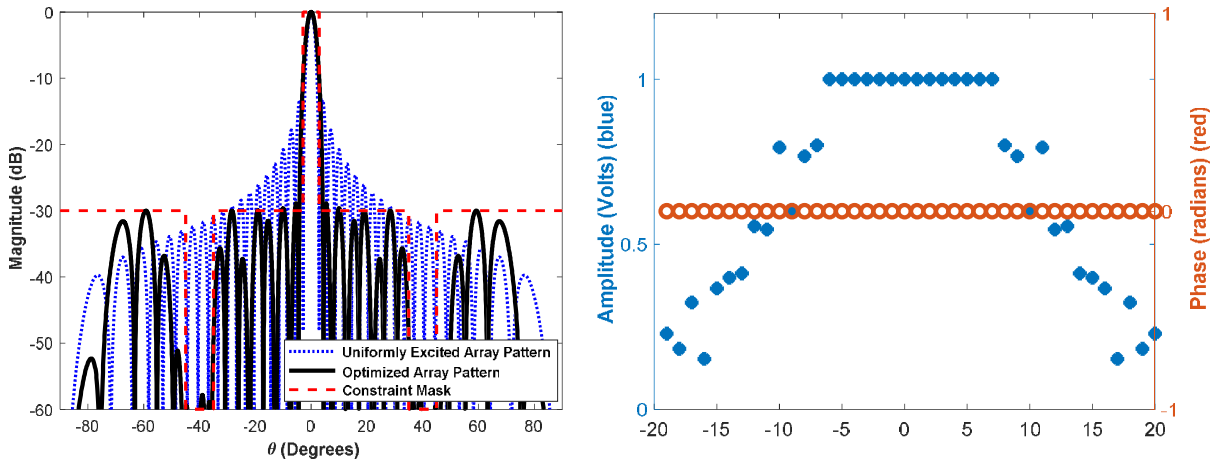

Figure 1. Array patterns and its corresponding taper weights for $M_1 = 7$, $M_2 = 13$, and $M_3 = 0$.

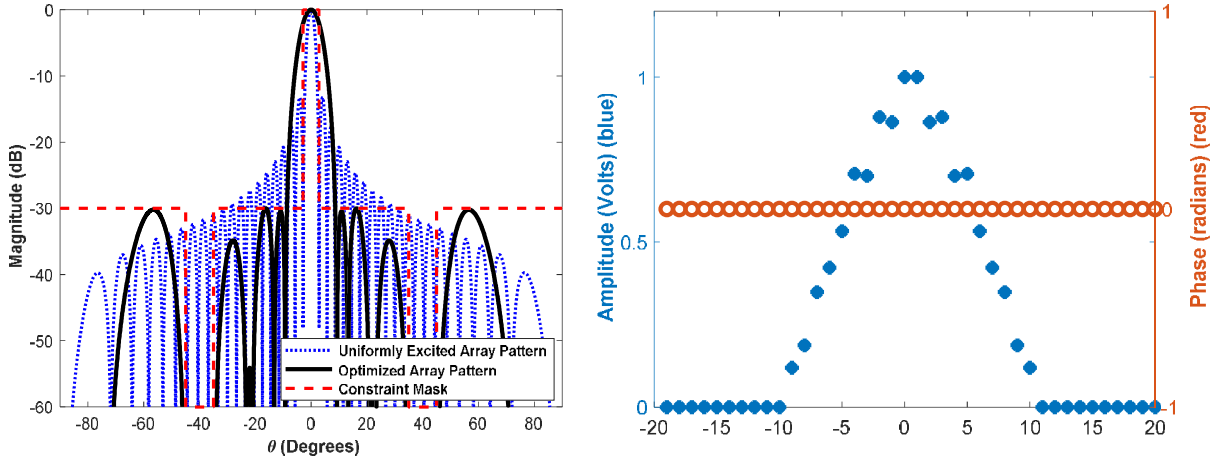

Figure 2. Array patterns and its corresponding taper weights for $M_1 = 1$, $M_2 = 9$, and $M_3 = 10$.

two symmetric wide steered nulls centered at $\theta = \pm 40°$ and ranged from $\theta = \pm 35°$ up to $\theta = \pm 45°$. Optimization result shows that each side of the considered array is portioned to $M_1 = 7$, $M_2 = 13$, and $M_3 = 0$ elements as shown in Fig. 1. This figure also shows the corresponding array pattern for the designed weights. For comparison purpose, the uniformly excited array pattern was also included in this figure. From this result, it can be observed that the first null to null beam width (FNBW) of the designed array is 9° which is a little wider than that of the uniformly excited array by 1.5°, and all of its sidelobes are below −30 dB. Also, the two desired nulls are accurately placed.

To switch the radiation pattern to wide mode and maintain the same SLL and steered nulls as in the previous example, the number of elements in each subset is determined as $M_1 = 1$, $M_2 = 9$, and $M_3 = 10$. Fig. 2 shows the resulting array pattern under such partitioned case. Here, it can be observed that the FNBW of such an array is 18.6° which is greatly wider than that of the pervious narrow beam pattern. Also note that all of its SLLs are still maintained below −30 dB, and the two desired nulls are within the required depth and width. Table 1 summarizes the performances of the above mentioned two tapered array designs.

Figure 3 shows another case of the resulting array pattern for $M_1 = 1$, $M_2 = 7$, and $M_3 = 12$ elements. Next, the variations of the taper efficiency, directivity, beam width, and the SLL for different numbers of the thinned elements in the outer subset region are illustrated in Table 2. In this table, the number of elements in the central subset region was set to $M_1 = 1$. From these results, it is

Table 1. Weights and performances of the tested arrays.

Designs	Subsets	Weights	Taper Efficiency	Directivity (dB)	SLL (dB)	FNBW (deg.)
Uniform Array	$M = 20$	1,1,1,1,1,1,1,1,1,1,1,1,1,1,1,1,1,1,1,1	1	28.21	−13.2	6.0
Design 1	$M_1 = 7$ $M_2 = 13$ $M_3 = 0$	0.16,0.23,0.26,0.21,0.29,0.43,0.38,0.57, 0.47,0.84,0.54,0.80,0.71,1,1,1,1,1,1,1	0.81	26.38	−30	9.0
Design 2	$M_1 = 1$ $M_2 = 9$ $M_3 = 10$	0,0,0,0,0,0,0,0,0,0.11,0.18,0.34,0.42, 0.53,0.70,0.70,0.87,0.86,1	0.4	20.23	−30	18.6
Design 3	$M_1 = 1$ $M_2 = 7$ $M_3 = 12$	0,0,0,0,0,0,0,0,0,0,0,0.04,0.04, 0.11,0.17,0.41,0.64,0.90,1	0.22	15.39	−31	42

Table 2. Performance of the designed array under different number of elements in the outer subset.

Performances	Tapered Array Pattern									
	Number of array elements per side = 20, $M_1 = 1$, M_2 and M_3 are variables									
	$M_3 = 0$	$M_3 = 2$	$M_3 = 4$	$M_3 = 6$	$M_3 = 8$	$M_3 = 10$	$M_3 = 12$	$M_3 = 14$	$M_3 = 16$	$M_3 = 18$
Taper Efficiency	0.85	0.75	0.67	0.56	0.5	0.41	0.22	0.22	0.1	0.06
Directivity (dB)	26.84	25.76	24.80	23.28	22.23	20.57	15.39	15.0	9.18	5.39
SLL (dB)	−30	−30	−30	−31	−30	−30	−31	−31	-	-
FNBW (deg.)	8.5	9.6	10.8	13	14.6	17.6	42	44.6	160	170

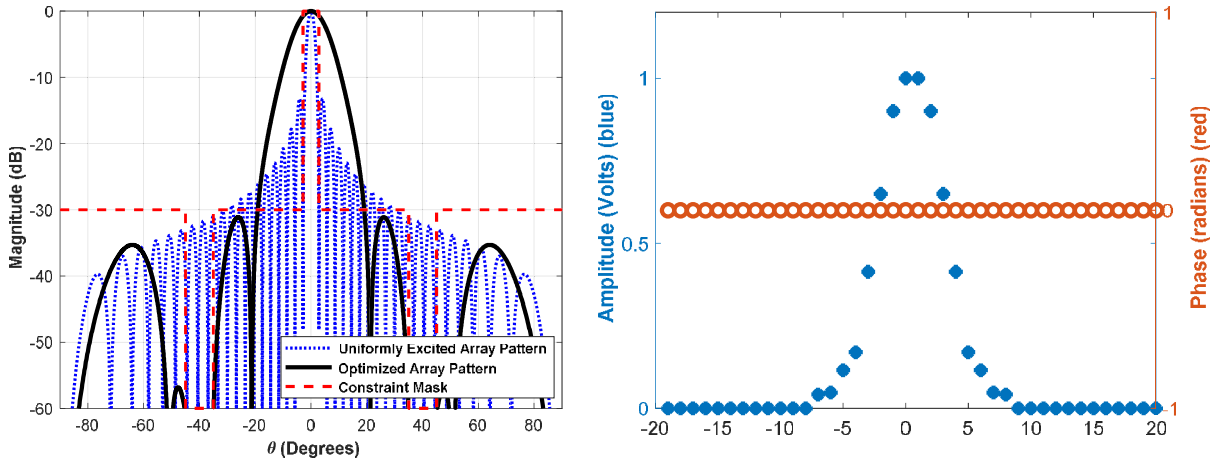

Figure 3. Array patterns and its corresponding taper weights for $M_1 = 1$, $M_2 = 7$, and $M_3 = 12$.

found that the directivity and taper efficiency get lower when increasing the number of outer thinned elements. In addition, the taper's width becomes narrower which results in a wider beam pattern. More importantly, the SLL and steered nulls are both maintained within the desired limits regardless of the thinned elements number. This is mainly because the proposed subset tapers have been designed without abrupt changes in the excitation amplitudes. The number of adaptive elements in the middle subset region controls the transition width between the thinned region and centered region.

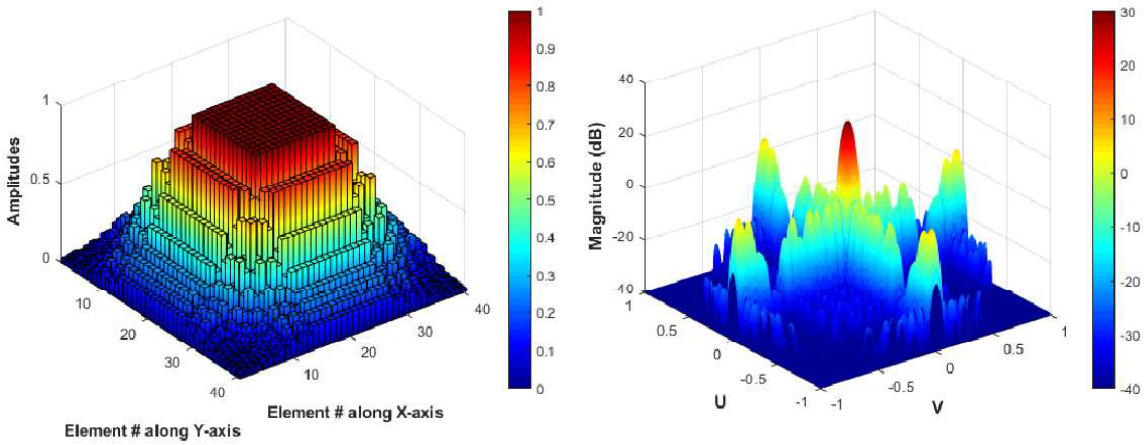

Figure 4. Planar beam-pattern and its corresponding taper weights for $M_1 \times M_1 = 7 \times 7$, $M_2 \times M_2 = 13 \times 13$, and $M_3 \times M_3 = 0 \times 0$ elements.

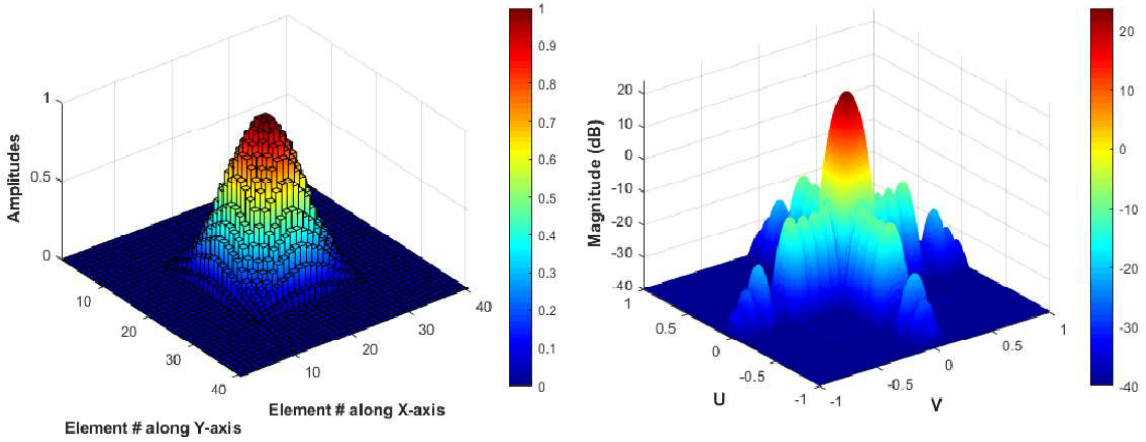

Figure 5. Planar beam-pattern and its corresponding taper weights for $M_1 \times M_1 = 1 \times 1$, $M_2 \times M_2 = 9 \times 9$, and $M_3 \times M_3 = 10 \times 10$ elements.

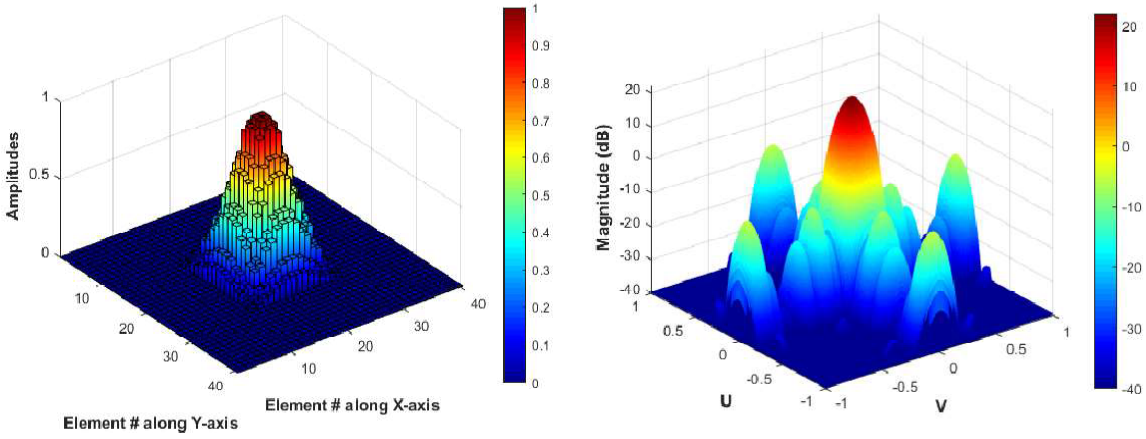

Figure 6. Planar beam-pattern and its corresponding taper weights for $M_1 \times M_1 = 1 \times 1$, $M_2 \times M_2 = 7 \times 7$, and $M_3 \times M_3 = 12 \times 12$ elements.

Finally, the proposed method was extended and applied to the square planar array of dimension 20×20 elements. Fig. 4 shows the optimized amplitude weights along with their corresponding beam-pattern for $M_1 \times M_1 = 7 \times 7$, $M_2 \times M_2 = 13 \times 13$, and $M_3 \times M_3 = 0$ elements. Fig. 5 shows the result for another case of $M_1 \times M_1 = 1 \times 1$, $M_2 \times M_2 = 9 \times 9$, and $M_3 \times M_3 = 10 \times 10$ elements, while Fig. 6 shows the results for $M_1 \times M_1 = 1 \times 1$, $M_2 \times M_2 = 7 \times 7$, and $M_3 \times M_3 = 12 \times 12$ elements. These figures satisfy the desired beam-patterns and prove the effectiveness of the proposed method for both linear and planar arrays.

4. CONCLUSIONS

From the demonstrated results, it has been found that the designed taper array have capability to easily switch between narrow and wide beam patterns by adaptively controlling the number of elements and their amplitudes in each subset region. Unlike other existing array tapers, the proposed taper has three different regions, namely, uniform, transit, and thinned regions with full adaptive control on their element excitation weights. The elements in the transit region play a major role in satisfying the required SLL and steered nulls, while the elements in the uniform and thinned regions control the beam widths of the resulting array patterns.

REFERENCES

1. Fernandez-Delgado, M., J. Rodriguez-Gonzalez, R. Iglesias, S. Barro, and F. Ares-Pena, "Fast array thinning using global optimization methods," *Journal of Electromagnetic Waves and Applications*, Vol. 24, No. 16, 2259–2271, 2010.
2. Oliveri, G., M. Donelli, and A. Massa, "Linear array thinning exploiting almost difference sets," *IEEE Transactions on Antennas and Propagation*, Vol. 57, 3800–3812, 2009.
3. Morabito, A. F., R. Palmeri, V. A. Morabito, A. R. Laganà, and T. Isernia, "Single-surface phaseless characterization of antennas via hierarchically ordered optimizations," *IEEE Transactions on Antennas and Propagation*, Vol. 67, No. 1, 461–474, Jan. 2019, doi: 10.1109/TAP.2018.2877270.
4. Mohammed, J. R., "Optimal null steering method in uniformly excited equally spaced linear array by optimizing two edge elements," *Electronics Letters*, Vol. 53, No. 13, 835–837, Jun. 2017.
5. Sayidmarie, K. and J. R. Mohammed, "Performance of a wide angle and wide band nulling method for phased arrays," *Progress In Electromagnetics Research M*, Vol. 33, 239–249, 2013.
6. Mohammed, J. R., "Synthesizing sum and difference patterns with low complexity feeding network by sharing element excitations," *International Journal of Antennas and Propagation*, Vol. 2017, 7 pages, Article ID 2563901, 2017.
7. Mohammed, J. R., "Thinning a subset of selected elements for null steering using binary genetic algorithm," *Progress In Electromagnetics Research M*, Vol. 67, 147–157, 2018.
8. Mohammed, J. R., "A method for thinning useless elements in the planar antenna arrays," *Progress In Electromagnetics Research Letters*, Vol. 97, 105–113, 2021.
9. Balanis, C. A., *Antenna Theory, Analysis and Design*, 4th Edition, Wiley, 2016.